Spatial Variation of Stable Water Isotopes in Fresh Snow along the Southside Slope of the “Chruez”, Praettigau Switzerland

Bachelor Thesis

2021

Institute of Geography

Hans Peter Pleisch / 18-114-207

Panyerstrasse 30

7243 Pany

hans.pleisch@students.unibe.ch

Advisor: Natalie C. Ceperley, Institute of Geography

University Bern

Table of Content

Acknowledgments .....

Summary .....

1 Introduction 1

1.1 Context 1

1.2 Introduction to Stable Isotopes 2

1.2.1 Definition and Notation of Isotopes 2

1.2.2 Stability of Isotopes 2

1.2.3 Isotope (abundance) Ratio and δ-Value 3

2 State of Knowledge 4

2.1 Equilibrium Fractionation 6

2.2 Kinetic Fractionation 6

2.3 Altitude Effect and Altitudinal Gradient 6

3 Goal, Research Question & Hypothesis 7

3.1 Goal 7

3.2 Research Question 8

3.3 Hypothesis 8

4 Study Site and Data 8

4.1 Site Description 8

4.2 Data 11

4.2.1 Snow Samples 11

4.2.2 Weather Stations and Meteorological Data 11

4.2.3 Temperature 12

4.2.4 Fresh Snow 14

4.2.5 Solar Radiation 14

4.2.6 Wind Direction and Wind Speed 15

5 Methods 16

5.1 Field Work 16

5.2 Lab Work 18

5.3 Statistical Analysis 18

6 Results 18

6.1 δ^{2}H-Values 19

6.2 δ^{18}O-Values 20

6.3 δ^{17}O-Values 22

6.4 GMWL and LMWL 23
6.5 Temperature 24
6.6 Snowfall Events 24
6.7 Solar Radiation 25
6.8 Wind Direction and Speed 25
7 Discussion 26
7.1 The Altitude Effect 26
7.2 Temperature 27
7.3 Snowfall Events 28
7.4 Solar Radiation 28
7.5 Wind Direction and Speed 28
7.6 Error Sources 29
7.6.1 Field Work 29
7.6.2 Lab Work 30
7.6.3 Meteorological Data 30
8 Conclusion 31
8.1 Future Research 31

Table of Figure

Figure 1: Possible distribution of $\delta^{2}H$ and $\delta^{18}O$-values (Beria et al., 2018) 5
Figure 2: Sampling Route (blue line) and sample locations (red markers). 10
Figure 3: Number of Samples per Altitude 11
Figure 4: Weather stations used for this bachelor thesis. From left to right; Schiers (green marker), St.Antoenien (yellow marker), Saas in Praettigau (blue marker) and Klosters Madrisa (orange marker) 12
Figure 5: Daily fresh snow measurements 14
Figure 6: Daily global radiation mean and total sunshine duration for each sampling day 14
Figure 8: Vial used for storing snow samples 16
Figure 7: Avalanche shovel and zip lock bag used for each sample run 16
Figure 9: Field notes made during sampling runs 16
Figure 10: Sampling run depicted as a flow chart 17
Figure 11: Cavity Ring Down Spectrometer (CRDS) used at the lab of the Institute of Geography at the University of Berne 18
Figure 12: $\delta^{2}H$-values 19
Figure 13: $\delta^{18}O$-values 21

Figure 14: $\delta^{17}O$-values....22
Figure 15: $\delta^{2}H$-$\delta^{18}O$ plot with their LMWL and GMWL....22
Figure 16: Daily $\delta^{18}O$-mean plotted against temperature....24
Figure 17: Daily fresh snow measurements from 01.03.2021 until 28.03.2021 plotted against daily mean $\delta^{18}O$-mean of each sampling day....25
Figure 18: Daily $\delta^{18}O$-slope plotted against daily mean global radiatio....26

Table Directory

Table 1: Sampling Locations....9
Table 2: Calculated mean temperature and temperature gradient for each sampling day....13
Table 3: Wind measurements taken from the weather station in Schiers....15
Table 3: δ-values of the water standards ANZO, EMEB and SAAS used to standardize my snow samples....19
Table 4: Linear regression results of the explanatory variable $\delta^{2}H$. In bold are the values, which are statistically significant....20
Table 5: Linear regression results of the explanatory variable $\delta^{18}O$. In bold are the values, which are statistically significant....21
Table 6: Linear regression results of the explanatory variable $\delta^{17}O$. In bold are the values, which are statistically significant....23
Table 7: Wind measurements from the weather station in Schiers in addition with the altitude gradient of each sampling day....26
Table 8: Deviations from the δ-values of the control samples to the reference samples....30

Acknowledgments

At this point I would like to thank all the people who have helped and supported me throughout the completion of this bachelor thesis. I would like to express my deepest thanks to my advisor Natalie C. Ceperley for all her great inputs and feedbacks, which helped me get on the right track while writing my thesis. I am also very grateful to the Institute of Geography in Bern for allowing me to borrow their equipment for me to use during my sampling runs and the use of their lab to analyse my snow samples.

A big thank you also goes to my colleague Manuel Rüdisühli, who has helped me out a lot, especially during the analysis of my snow sample data. Finally, I would like to thank my friends Nikola Nenad, Dario Nespolo, Harry Braillard, Sandro Grass, Gianni Stiffler, Carina Oberhaensli and Vanessa Amez-Droz for taking their time to read my bachelor thesis and pinpointing any grammatical errors or ambiguities.

Summary

This bachelor thesis concerned itself with the composition of $\delta^{2}H$ (or deuterium), $\delta^{18}O$ and $\delta^{17}O$ in fresh snow. Stable water isotopes have been proven to be useful tracers for hydrological processes, such as air mass sources of regional precipitation or the residence time of snowmelt in a catchment (Beria et al., 2018). Whereas different isotopic compositions of precipitation in the form of rain is well documented for different environments in networks such as the NISOT (The Swiss National Network for the Observation of Isotopes in the Water Cycle), the same knowledge about snow is more limited due to the influences of different isotope fractionation processes and lack of onsite snow accumulation and melt observation (Cooper, 1998; Michelon et al., 2018). The aim of this thesis was therefore to analyse and characterize the spatial variability of $\delta^{2}H$, $\delta^{18}O$ and $\delta^{17}O$ in freshly fallen snow. This was done by sampling fresh snow on six different snowfall events in the month of March over an elevation gradient of 1000m along the southside slope of the mountain Chruez. ^{2}H throughout four sampling days had δ-values ranging from −50‰ to −70‰, with two days being more depleted in ^{2}H, showing δ-values from −80‰ down to −160‰. ^{18}O showed the same pattern where of six, four days showed similar δ-values ranging from −8‰ to −12‰ and two days with a stronger depletion of the isotope with δ-values ranging from −14‰ to −20‰. It is known that the enrichment of ^{17}O in a water molecule is about half of ^{18}O, which was also seen in the results of this thesis (Nyamgerel et.al, 2021).

In this thesis, two out of six sampling days were examined with statistically significant positive altitude gradients of 0.19‰/100m and 0.64‰/100m for $\delta^{18}O$. Additionally, on one of the six sampling days, a statistically significant negative altitude gradient of −0.15‰/100m was observed. The altitude gradients for $\delta^{17}O$ were about half of $\delta^{18}O$. Two statistically significant positive and one negative altitude gradients for $\delta^{2}H$ were observed during the same days with lapse rates of 1.7‰/100m, 5.5‰/100m and −1.25‰/100m. Having both positive and negative altitude gradients was attributed to the varying amounts of solar radiation and wind direction during different sampling days. However, further research must be done in order to make a valid statement, since additional factors such as water vapor pressure, turbulent fluxes in the air and relative humidity strongly affect fractionation of stable water isotopes.

1 Introduction

1.1 Context

Variations in the isotopic composition of precipitation have been proven to be useful for hydrological studies, groundwater management and protection, determination of groundwater origin and age, and calibration of flow and transport modelling since the late 1950s and early 1960s. Networks such as “The Swiss National Network for the Observation of Isotopes in the Water Cycle (NISOT)” have been observing stable water isotopes in precipitation, surface water (river) and groundwater since 1992 (Galewsky et al., 2016; Schürch et al., 2003).

Stable water isotopes are commonly used to trace the source of water and its flow pathways (Vreča & Kern, 2020). Since stable water isotopes are inherent to the water molecule, they are also considered ideal tracers to identify changes in the hydrological cycle on a global, regional, and local scale (Kern et al., 2014). For example, stable water isotopes have been used to trace airmass sources of regional precipitation, how different water bodies relate to each other, to quantify the extent of evaporation or to identify the residence time of snowmelt in a catchment (Peng et al., 2015; Dietermann & Weiler, 2013). Since stable water isotopes are constituents of the water molecule, they are strongly dependent on meteoric processes, which leads to different isotopic signatures in water depending on the environment and therefore reflect the seasonal variation of the temperature and precipitation, as well as the geographical latitude and the altitude of the location where the isotopes were measured (Schürch et. al., 2003).

The isotope compositions of precipitations in the form of rain are well documented for different environments in networks like the NISOT. However, considering the lack of onsite snow accumulation and melt observation, the same information is more limited for precipitations in the form of snow (Michelon et al., 2018). This can also be attributed to the more complicated sampling process and modelling of isotopic composition of snowmelt water due to different isotope fractionations during, formation, accumulation and ablation of snow and phase changes amidst snowmelt. There is also still a lack of knowledge concerning flow paths and water partitioning in snow dominated, high-elevation, alpine environments, which can be related to the poor understanding of spring snowmelt processes. Furthermore, each snowpack varies in its isotopic composition due to the variation of isotopic content of individual precipitation event (Cooper, 1998). However, with a more detailed knowledge about isotopic composition of snow, one could better understand hydrological processes such as the snowmelt contribution to streamflow or residence time of snowmelt in a catchment (Dietermann & Weiler, 2013; Ceperley et. al, 2020).

1.2 Introduction to Stable Isotopes

The following chapters will provide background information regarding stable water isotopes including a definition of isotopes, clarification of stable, and notes about notation.

1.2.1 Definition and Notation of Isotopes

Atoms consist of a nucleus, which is kept together by strong forces between the nucleons (protons and neutrons). The sum of the protons and neutrons of a nucleus equals the mass number (Mook, 2001). Atoms of the same element, which have different numbers of neutrons, are called isotopes (Galewsky, 2016). All of the different combination of isotopes, which can compose a molecule, are called isotopologues. To differentiate the various kinds of specific nucleus in written form, the following notation has been established:

$$^{A}_{Z}X_{N}$$

The letter "X" stands for the specific element, which is accompanied by the number of protons (Z) and neutrons (N) and the sum of protons and neutrons (A). Since the chemical property is mainly dependent on the numbers of electrons, which is equal to the number of neutrons, the notation ^{A}X is sufficient to define the nuclide (Mook, 2001).

1.2.2 Stability of Isotopes

Instabilities within isotopes are attributed to the excess number of protons or neutrons, which cause radioactive decay and therefore induce a diminishing effect on the concentration of the isotopic concentration of a molecule. These types of isotope are also referred to as unstable or radioactive isotopes (Mook, 2001). Isotopes, which have even numbers of protons or/and neutrons, are generally stable, and therefore have a larger natural occurrence. This phenomenon is also referred to as the "Oddo-Harkins" rule. A second rule, which applies to the stability of an isotope, is the so-called symmetry rule. The rule states when the number of protons is or is close to equal to the number of neutrons, hence a neutron-to-proton ration of or close to 1, the isotope is more stable (Hoefs, 2015).

The focus of this bachelor thesis lies on different isotopes of hydrogen and oxygen, as they compose the water molecule (H_2O). In nature, stable hydrogen exists as the two isotopes ^{1}H, ^{2}H (or D), whereas stable oxygen occurs as ^{16}O,^{17}O and ^{18}O (Beria et al., 2018). According to Sharp (2017), there are nine possible isotopologues of water. However, of these nine isotopologues, only the four isotopologues ($H_2{}^{16}O$, $H_2{}^{17}O$, $HD^{16}O$, and $H_2{}^{18}O$) are sufficiently abundant in nature, to have a significant impact to the isotope geochemistry.

The difference in the numbers of neutrons across the various isotopes of an element, leads to different mass numbers. For example, the hydrogen isotope deuterium (^{2}H) has one neutron and one proton, whereas tritium (^{3}H) has two neutrons and one proton, which results in a mass approximately twice as large compared to deuterium (Galewsky, Kendall). According to Mook (2001) the mass difference influences the following two physical and chemical properties of an isotopic compound (e.g., a water molecule containing different isotopes of the same element):

1) Molecules constituted of heavier isotopes have, due to their larger mass, a lower mobility compared to molecules constituted of lighter isotopes. Consequently, heavier molecules have a lower diffusion velocity, which leads to lower collision frequencies. Therefore, heavier molecules react slower, compared to light molecules.
2) Molecules constituted of heavier isotopes generally have higher binding energies and consequently need more energy to be released from the compound

1.2.3 Isotope (abundance) Ratio and δ-Value

The abundance of an isotope is described as a ratio (R) of the concentration of the heavy (rare) isotope relative to the light (abundant) isotope (Mook, 2001).

$$R = \frac{abundance\ of\ rare\ isotopes}{abundance\ of\ abundant\ isotopes} = \frac{^2H}{^1H} \qquad \textit{(Formula 1)}$$

However, isotope ratios are not generally expressed in absolute numbers. The stable isotopic composition of a sample is generally reported as a δ-value (spelled and pronounced as "delta"), which is the deviation of the isotope ratio of a sample (R_x) relative to that of a standard of known composition (R_s) (Mook, 2001; Kendall & McDonnell, 1998). δ-values are calculated as followed:

$$\delta\ (\text{in}\ ‰) = \left(\frac{R_x}{R_s} - 1\right) \times 1000 \qquad \textit{(Formula 2)}$$

More specific to this bachelor thesis, the stable isotopic composition of water is expressed through the deviation of the isotope ratio of the sample in question (R_{Sample}) to that of the Vienna Standard Mean Ocean Water (VSMOW) by the International Atomic Energy Agency (IAEA) (R_{VSMOW}) (Beria et al., 2018):

$$\delta^2H\ or\ \delta^{18}O = \frac{R_{Sample} - R_{VSMOW}}{R_{VSMOW}} \times 1000 \qquad \textit{(Formula 3)}$$

In total, there are four different ways to interpret and compare the δ-values of two different isotopes, which are stated by Kendall and McDonnel (1998):

1) high vs. low values
2) more/less positive vs. more /less negative (e.g., -10‰ is more positive than -20‰)
3) heavier vs. lighter (the "heavy" material is considered the one with higher δ-values)

4) enriched vs. depleted (e.g., higher (or less negative) δ-values indicate samples "enriched" in heavier isotopes, lower (or more negative) δ-values indicate samples "depleted" in heavier isotopes)

2 State of Knowledge

As mentioned in 1.2.2, in nature, stable hydrogen exists as the two isotopes ^{1}H, ^{2}H (or D), whereas stable oxygen occurs as ^{16}O,^{17}O and ^{18}O, also called the triple oxygen isotope system. For tracing purposes in isotope hydrology, ^{2}H and ^{18}O are the most used and are considered heavy isotopes (Beria et. al, 2018; Nyamgerel et. al, 2021). The composition of ^{2}H and ^{18}O in waters is heavily dependent on meteoric processes, which leads to a characteristic isotopic signature (Schürch et al., 2014). ^{17}O has been considered as an additional tracer due to the isotope being a proxy for humidity at the region of evaporation, whereas the composition ^{2}H and ^{18}O are more dependent on temperature (Berman et al., 2013). This results from the fact that ^{2}H and ^{18}O are considered heavy isotopes, whereas ^{17}O is considered as a lighter isotope and is therefore more likely to evaporate. Additionally, the enrichment of ^{17}O in a water molecule is about half of ^{18}O. Contrarily, ^{2}H and ^{18}O, being heavy isotopes, tend to condensate into the liquid or solid phase. Despite several studies investigating the potential use of ^{17}O for a deeper understanding of the hydrological cycle, there is still little knowledge on how the processes, which control the spatiotemporal distribution of ^{17}O, work (Nyamgerel et.al, 2021). Furthermore, there has been little research done, which dealt with the use of ^{17}O in snow hydrology. This can be related to the difficulty of measuring ^{17}O concentrations in water (Beria et al., 2018). What has been determined is that atmospheric moisture, precipitation, surface water and groundwater are mostly depleted in the heavy isotopes ^{18}O, ^{2}H and ^{17}O, compared to ocean water. This is due to the fractionation processes taking place in these waters (Schürch et al., 2014). During an isotope fractionation, the isotopic composition of an element changes, which means that the relative abundance of heavier and lighter isotopes differs after a phase change process. As a rule, isotope fractionation decreases with increasing temperature and humidity (Mook, 2001; Putman et al., 2021). There are two main types of isotope fractionation. The type of fractionation taking place is determined by the process, which is currently present. Fractionation occurs either under equilibrium (equilibrium fractionation) or nonequilibrium conditions (kinetic fractionation) (Beria et al., 2018). Both fractionation processes will be furtherly discussed in chapter 2.1 and 2.2.

According to Kong and Pang (2016), the heavy isotope concentration in precipitation declines at higher altitudes in comparison to lower altitudes. Therefore, a negative stable isotope-altitude gradient is expected on the windward side of a mountain. This "altitude Effect" will be discussed in detail in chapter 2.3, as it plays a major role in this bachelor thesis. Additionally, the isotope composition in precipitation varies in between seasons, due to its correlation to air temperature and water vapour pressure. ^{18}O and ^{2}H reach their highest δ-value generally during summer and autumn, caused through the high air temperature and vapour pressure. On the other hand, ^{18}O and ^{2}H reach their lowest δ-value during the winter season, when the air temperature and vapour pressure are low (Schürch et. al, 2003). Thus, rain tends to be more enriched in heavier isotopes than snowfall (Beria et al., 2018). The

concentration of ^{2}H and ^{18}O is both heavily determined by the fractionation process present. Furthermore, since both ^{2}H and ^{18}O are part of the same water molecule undergoing transformation, their ratio fall along a line, which results in the following equation: $\delta^{2}H = 8\delta^{18}O + 10$. This relationship between the ratio of these two water isotopes is also referred to as the global meteoric water line (GMWL) and was defined by Craig (1961). But since stable water isotopes are affected differently during kinetic fractionation, due to dependence on the mass of the isotope, δ-values deviate from the GMWL (or LMWL (Local)) (Fig. 1) (Beria et al., 2018; Kendall & McDonnell, 1998). A slope of 8 was defined due to the approximate ratio of the equilibrium fractionation factors of the stable isotopes of H and O at 25-30°C (Kendall & McDonnel, 1998). The value of 8 can therefore change depending on the temperature range equilibrium fractionation takes place locally. The intercept value 10 represents the deuterium excess parameter and is defined as $d = \delta^{2}H - 8\delta^{18}O$. Deuterium excess is also used as tool to identify nonequilibrium processes and is characterized with a high d-value (Putman et al., 2019). Putman et al.'s evaluation of various LMWL's across the globe showed that for snow, a high d-value occurs when it is formed from mixed-phase clouds, which are clouds consisting of supercooled cloud droplets and ice.

Meteoric water lines are therefore strong tools for evaluating hydroclimatic processes and assessing the relationship between $\delta^{2}H$ and $\delta^{18}O$ (Putman et al., 2019; Beria et al., 2018). However, since certain parameters vary on a local scale (e.g., slopes or intercept of precipitation), local meteoric water lines (LMWL or MWL) are generally used to assert the relationship between $\delta^{2}H$ and $\delta^{18}O$ (Beria et al., 2018). One has to keep in mind that most available LMWLs are representative for precipitation in the form of rain due to the reasons mentioned in chapter 1.1.

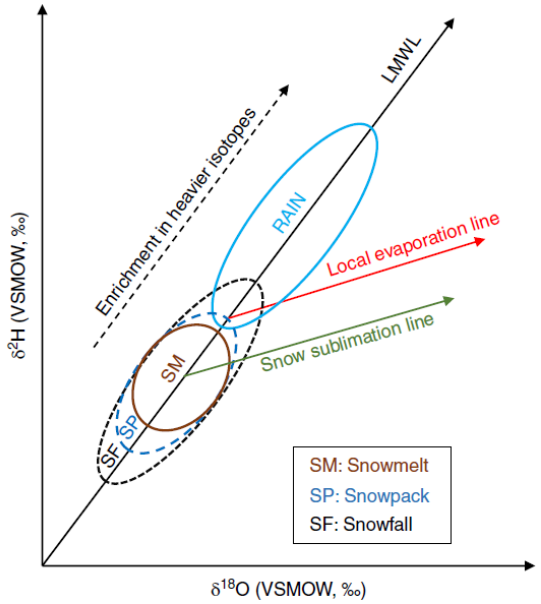

Figure 1: Possible distribution of $\delta^{2}H$ and $\delta^{18}O$-values (Beria et al., 2018)

2.1 Equilibrium Fractionation

Equilibrium fractionation defines a redistribution of isotopes of an element between various species or compounds. One must keep in mind that an exact equilibrium fractionation only occurs in a closed, well-mixed system at chemical equilibrium. During equilibrium fractionation the forward and backward reaction rate of any isotopes are the same. However, that does not mean that the isotopic composition of two compounds is identical, but merely the ratio of different isotopes in each compound are constant for a particular temperature. When the current process indicates an equilibrium fractionation, for example condensation, the liquid phase becomes more enriched in heavier isotopes (e.g., ^{2}H and ^{18}O), whereas lighter isotopes remain in the vapor phase. Due to this process, precipitation events near coastal region are less depleted in heavy isotopes, whereas air masses moving across continents are becoming more depleted in heavy isotopes due to the loss of water by rainout and the fact that the liquid phase is enriched in heavy isotopes relative to the vapor phase. This is also referred to as the "Continental Effect" (Kendall & McDonnel, 1998).

2.2 Kinetic Fractionation

Unlike with equilibrium fractionations, the forward and backward reaction rate of kinetic (or non-equilibrium) fractionations are not identical. When kinetic fractionation is taking place, such as evaporation, the δ-value of ^{2}H and ^{18}O in the vapor decreases, while the remaining liquid is proportionately enriched in the heavy isotopes ^{2}H and ^{18}O. However, kinetic fractionation affects changes in the δ-value of ^{2}H stronger than ^{18}O in the vapor phase compared to equilibrium fractionation, which leads to a deviation from the meteoric water line (see chapter 2).
Snow sublimation is an important kinetic fractionation, which influences the isotopic composition of accumulated snow. It influences the isotopic composition by enriching the top layer of a snowpack in heavier isotopes (Beria et al., 2018). This form of kinetic fractionation is caused by differences in vapor pressure between surface snowpack layer and the surrounding atmosphere, warm temperatures, turbulent fluxes in the air, wind speed and solar radiation (Gustafson et al., 2010).

2.3 Altitude Effect and Altitudinal Gradient

The "Altitude Effect" occurs when equilibrium fractionation (e.g., condensation) processes are present. For this thesis specifically, "Altitude Effect" plays an important role in the isotopic composition of the fresh snow. As mentioned already in 2.2, the heavy isotope concentration in precipitation declines at higher altitudes in comparison to lower altitudes. This effect happens due to the preference of heavy isotopes during condensation. With decreasing cloud condensation temperature, and therefore increased elevation, the isotopic fractionation increases, leaving the condensate less and the remaining vapor more depleted in heavier isotopes (Beria et al., 2018). The effect occurs in this manner as far as orographic precipitations is concerned (Ambach et al., 1967). Additionally, this effect is also

heavily dependent on the parent condensing vapor and its evolution and therefore cannot be entirely separated from the "Continental Effect" (see chapter 2.1) (Kendall & McDonnel, 1998). The "Altitude Effect" is often expressed in the form of an "isotopic lapse rate" measured in per mil (‰). It showcases the change in δ^2H and $\delta^{18}O$ per 100m of elevation in the precipitation. However, the lapse rates can differ significantly, as it is heavily dependent on the moisture content of the air mass (Kumar et al., 2010). For the heavy isotope ^{18}O, the isotopic lapse rate generally varies between -0.1‰ and -0.6‰/100m in altitude. As for ^2H, the effect shows very different rates globally. In the coastal region of the western United States, the "Altitude Effect" showed an isotopic lapse rate of -4‰/100m, whereas in S.W Germany -2.5‰/100m and in Chile a range from -1‰/100m to -4‰/100m (Gat et al., 2001). A study conducted in the Eastern Alps by Dietermann and Weiler (2006) showed an altitude effect of δ^2H of fresh snow on north-facing slopes, ranging between -2.6‰/100m and -0.7‰/100m. Dietermann and Weiler additionally surveyed a south-facing slope, which showed a wide altitude gradient, ranging from -1.6‰/100m to -6.2‰/100m. The study also showed results with a positive altitude gradient of δ^2H in snow samples collected from south-facing slopes, which ranged from 0.2‰/100m to 3.1‰/100m.

Since the heavy isotope concentration declines at higher altitudes, a negative altitude gradient is generally expected. However, as seen in the study conducted by Dietermann and Weiler, there were also instances, where the isotopic lapse rate was reversed. Hence, the heavy isotope concentration in precipitation increased in higher altitudes and therefore shows a positive altitude gradient. Such a behaviour was also observed when Moran et al. (2007) conducted a study about the altitude gradient for the stable isotope ^{18}O on the leeward slope of the Canadian Rocky Mountains. Moran et al. argue that such an inverse altitude gradient occurred due to post-depositional modification, secondary moisture sources, which describes the fast mixing of low-altitude and high-altitude moisture in a column of convective precipitation or turbulent mixing of air masses on the leeward side of the mountain. Kong & Pang (2016) furtherly state that moisture recycling can cause a positive isotope gradient. In addition, positive isotope gradients can occur when evaporation and sublimation processes took place, along with snow drift from higher to lower altitudes (Moser & Strichler, 1974; Beria et al., 2018). Zongxing et al. (2015) observed a positive isotope gradient on the Shiyi glacier, with the assumption that it could be explained by the melting of the newly deposited snow.

3 Goal, Research Question & Hypothesis

3.1 Goal

Available data on the isotopic composition of snow, as mentioned in 1.1, is a valuable source to determine its effect on the hydrological cycle in the given area. However, the time intensive sampling process and modelling of isotopic composition due to fractionation processes, have made it difficult to establish a proper database. By sampling fresh

snow, the impact of the fractionation processes on the isotopic composition on snow can be minimized. Therefore, the goal of this thesis is to gather data with an appropriate sampling procedure and to analyse and characterize the isotopic composition of fresh fallen snow. These results should then also contribute to the existing research on the spatial variation of the isotopic composition of fresh snow.

3.2 Research Question

The following research question will be answered in this bachelor thesis:

- How does the composition of ^{18}O, ^{2}H and ^{17}O in snow vary in spring in the Eastern Alps according to elevation?
- How have the meteorological conditions influenced the isotopic composition of snow during my sampling runs?

3.3 Hypothesis

- Based on the altitude effect, I expect that the concentration of heavy isotopes ^{18}O, ^{2}H and ^{17}O will be more depleted in higher altitudes compared to lower altitudes and therefore shows a negative isotope-altitude gradient.
- Meteorological conditions prior and during the snowfall event, such as duration, temperature, solar radiation, wind direction and wind speed will have different impacts in the altitude gradient and isotopic composition of my snow samples, as they influence isotopic fractionation.

4 Study Site and Data

4.1 Site Description

All the snow was sampled on the south-facing slope of the mountain “Chruez”, located in the valley Praettigau (Fig.2). The “Chruez” belongs to the mountain range “Raetikon”, which lies on the western edge of the Eastern Alps close to the boarder to Austria and Italy. The whole study site ranged from the villages Luzein to Pany, with the lowest point being “Prif” at 1000m.a.s.l and the highest point being “Alpbueel” at 1970m.a.s.l. Each sampling location was given an abbreviation, where the lowest point was assigned the number “1” up to the highest point having the assigned number “11”. The letter X represents the sampling run. At some point during the sampling runs, control samples were planned to be collected, which were labelled the same as the reference sample but with the addition of the word “Control” (Tab. 1).

Within this site, eleven snow samples per sampling run were planned to be taken every altitudinal difference of 100m over an altitude gradient of 970m. All the samples were collected on open fields except for sample SX.6 and SX.10, which were located on slopes with a lesser steepness than 30°. The sample locations were placed in such a way, that any foliage or coniferous trees were prevented. This was important as precipitation intercepted by canopies enriches snow in heavier isotopes, which would then falsify my results (Beria et al., 2018). I also took into consideration that the sampling locations must not be near roads, as it influences temperature. Furthermore, exhaust fumes and plowing from cars might have an impact on the snow I sampled.

Name	**Abbreviation**	**Location Name**	**Altitude [m]**	**Coordinates (CH1903+/LV95)**
Sample 1	SX.1	Prif	1000	2'777'481 / 1'199'251
Sample 2	SX.2	Mittelberg	1100	2'777'291 / 1'199'635
Sample 3	SX.3	Maliet	1200	2'777'501 / 1'199'912
Sample 4	SX.4	Gueggelstein	1300	2'777'368 / 1'200'233
Sample 5	SX.5	Maiensaess	1400	2'777'209 / 1'200'659
Sample 6	SX.6	Schurli	1500	2'777'243 / 1'200'986
Sample 7	SX.7	Choechleri	1600	2'777'821 / 1'201'372
Sample 8	SX.8	In der Schwarzae	1700	2'777'517 / 1'201'542
Sample 9	SX.9	Chlei Tschuoggeri	1800	2'777'363 / 1'201'850
Sample 10	SX.10	Gauis	1900	2'777'009 / 1'202'021
Sample 11	SX.11	Alpbueel	1970	2'776'991 / 1'202'181
Sample X	SX. X / Control	-	-	-

Table 1: Sampling Locations

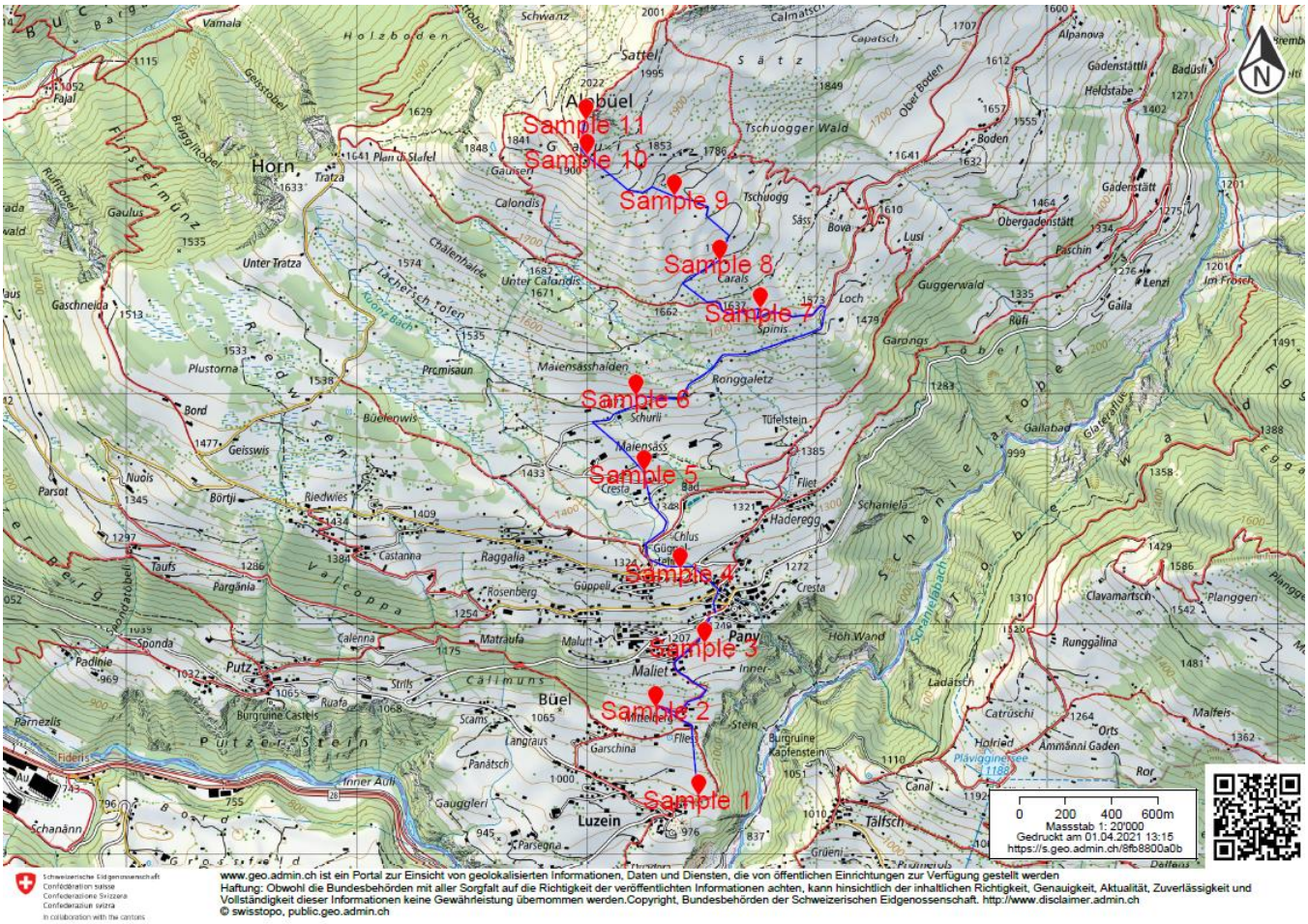

Figure 16: Sampling Route (blue line) and sample locations (red markers).

4.2 Data

4.2.1 Snow Samples

In total, 54 snow samples were collected of which 9 were control samples. However, due to the difference in altitude, the number of samples varied for some locations, since snow did not always fall in lower elevations (Figure 3). Additionally, due to safety regulations, there were instances where gathering samples in higher elevations was not

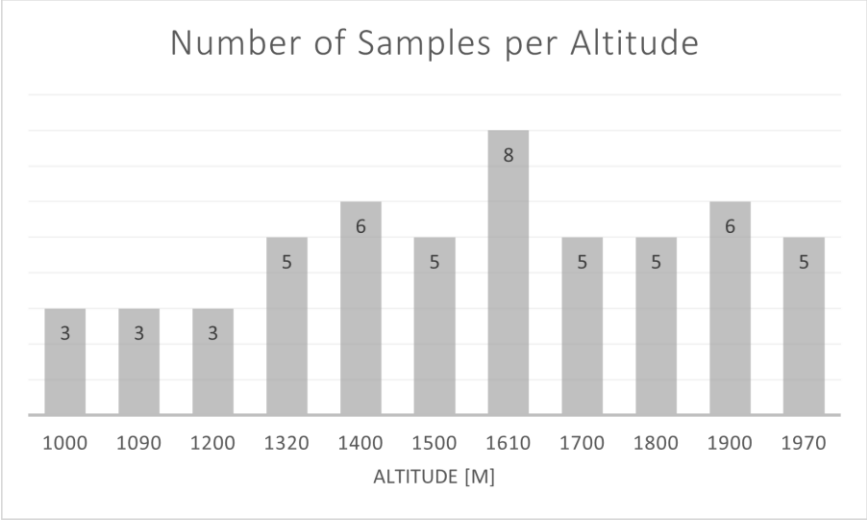

Figure 3: Number of Samples per Altitude

possible. The snow sample were collected on the six dates: 05.03.2021, 08.03.2021, 12.03.2021, 15.03.2021, 22.03.2021 and 27.03.2021. All samples were collected within 24 hours after a fresh snowfall occurred. The only requirement, which had to be met for me to go collect samples was that at least 1cm of fresh snow must had fallen. The snow samples were collected from the altitude 1000m.a.s.l up to 1970m.a.s.l. and were analysed on the composition of the stable water isotopes ^{18}O, ^{2}H and ^{17}O. In order to evaluate the data of the three isotopes, the collected snow was analysed in reference to three different water standards ANZO, EMEB and SAAS.

4.2.2 Weather Stations and Meteorological Data

In addition to my field notes, meteorological data was extracted through IDAWEB, which provides access to the archive data of MeteoSwiss' ground level monitoring network. The meteorological data should provide further insight into what might have influenced the δ-values of my snow samples on the days they were sampled. Meteorological data about daily solar radiation, air temperature, wind direction and wind speed were used for the further analysis of my results, since they are factors, which heavily influence isotopic fractionation processes. The meteorological data was gathered from the four weather stations (Fig. 3) in Schiers (626m.a.s.l), St.Antoenien (1510m.a.s.l), Klosters Madrisa (2160m.a.s.l) and Saas in Praettigau (988m.a.s.l). The meteorological data from Schiers and Klosters Madrisa were measured through automated weather stations set up by MeteoSwiss, whereas

the weather station in Saas in Praettigau was set up by MeteoGroup. Measurements coming from the weather station St.Antoenien were provided by the Snow Avalanche Institute in Davos (SLF). I was forced to use weather stations located outside of my sampling location, since there were not any available within my study site. The weather stations Schiers, Saas in Praettigau and Klosters Madrisa were selected because they have a south-facing exposition, which makes the data more applicable to my study site in comparison to other weather stations in the valley. However, despite it lying on the eastern side of the mountain Chruez, I also included the weather station in St.Antoenien, since it was the nearest and was the only weather station, which had fresh snowfall measurements within the altitude range of my study site.

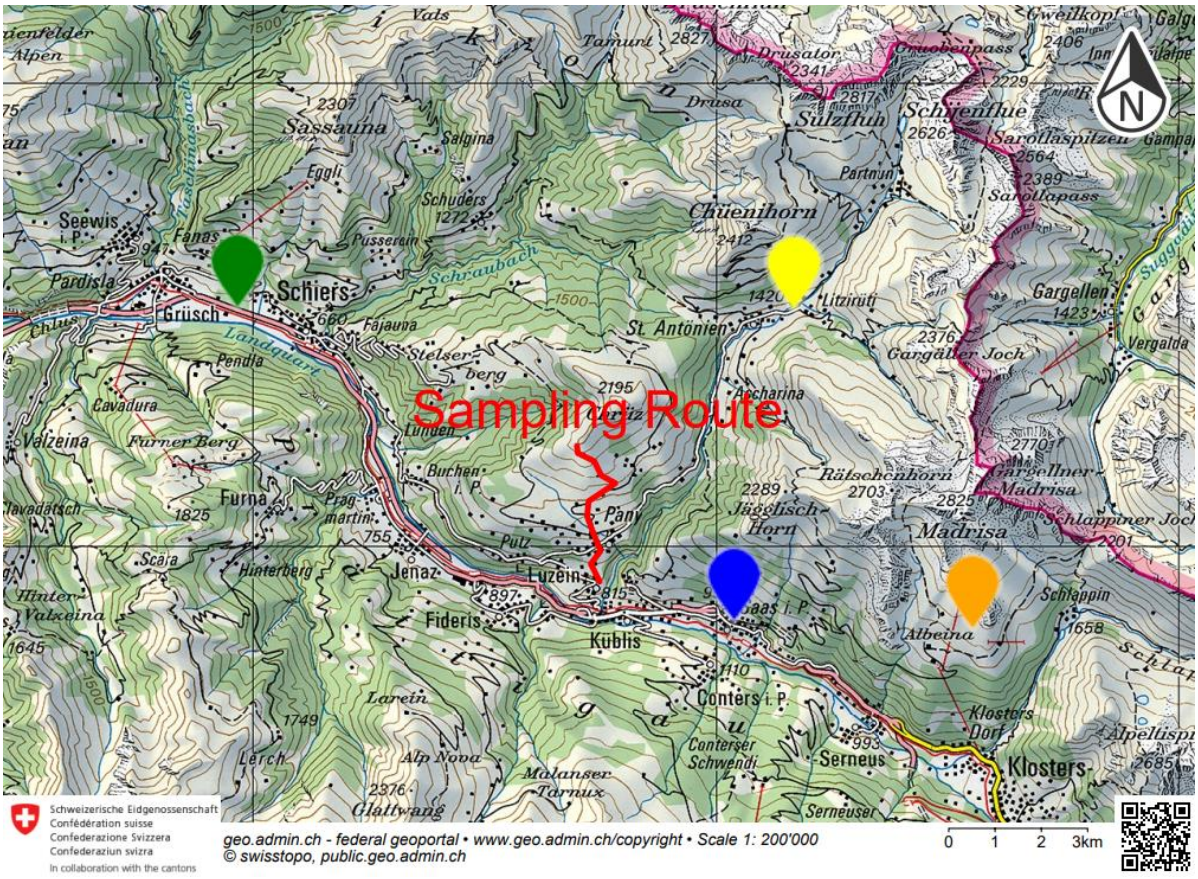

Figure 4: Weather stations used for this bachelor thesis. From left to right; Schiers (green marker), St.Antoenien (yellow marker), Saas in Praettigau (blue marker) and Klosters Madrisa (orange marker)

4.2.3 Temperature

Temperature measurements were extrapolated from the fore mentioned weather stations. This was done by calculating a temperature gradient (T_G) with the mean temperature of the stations Klosters Madrisa and Saas in Praettigau. Since Klosters Madrisa is located at a higher altitude than Saas in Praettigau, the mean temperature of Saas in Praettigau (T_S) was subtracted from the mean temperature of Klosters Madrisa (T_K). The difference was then divided by the altitude difference (Z_D), in this case 1534m, and then multiplied by the sampling frequency

(S_{freq}), which was every 100m in elevation gain, for the purpose of receiving a temperature gradient per 100m. This was done for each sampling day separately and is showcased in the following formula.

$$T_G = \frac{(T_K - T_S)}{Z_D} \times S_{freq} \quad \textit{(Formula 4)}$$

After calculating the temperature gradient (T_G), I used the hourly temperature measurements of Klosters Madrisa (T_{HK}) from my MeteoSwiss data and aligned them with the timestamp I wrote down in my notes when I collected my snow sample. Meaning, that the calculated mean temperature of each sampling days only accounts for the time I was outside on my sampling run and not for the whole day. When calculating the temperature of my sampling location (T_{SL}), I had to account for the altitude difference (Z_D), which I then multiplied with the temperature gradient of the respective sampling day. The following formula and table (Tab.3) show how I adapted the measured temperature of the weather station to the sample location and the respective mean temperature and temperature gradient of each sampling day.

$$T_{SL} = T_{HK} + (T_G \times Z_D) \quad \textit{(Formula 5)}$$

	05.03.2021	**08.03.2021**	**12.03.2021**	**15.03.2021**	**22.03.2021**	**27.03.2021**
Mean Temperature [C°]	-1.12	0.38	-1.96	-4.28	-3.23	0.54
Temperature Gradient [°/100m]	0.56	0.56	0.64	0.57	0.7	0.49

Table 2: Calculated mean temperature and temperature gradient for each sampling day

4.2.4 Fresh Snow

Daily fresh snow measurements were taken from the weather station in St.Antoenien. Since the isotopic composition of precipitation generally becomes more depleted in heavier isotopes upon the start of the snow or rain event (Beria et al., 2018), fresh snow measurements were used in this thesis in order to investigate the effect on my snow samples. Additionally, fresh snow was measured from 06UTC until 06UTC the following day, which is why I also had to take the measurements from the day prior to my sampling run into account. Figure 3 illustrates the fresh snow measurements from the 1st until the 28th of March.

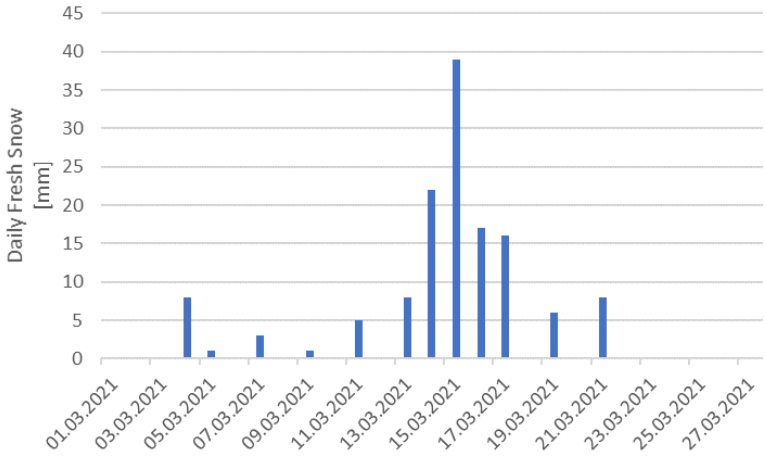

Figure 5: Daily fresh snow measurements

4.2.5 Solar Radiation

Measurements for global solar radiation was exclusively used from the weather station located in Saas in Praettigau. As mentioned in chapter 2.2., solar radiation contributes to the process of kinetic fractionation and therefore may have had an impact on the composition of stable water isotopes in snow. The following figure (Fig. 6) depicts the

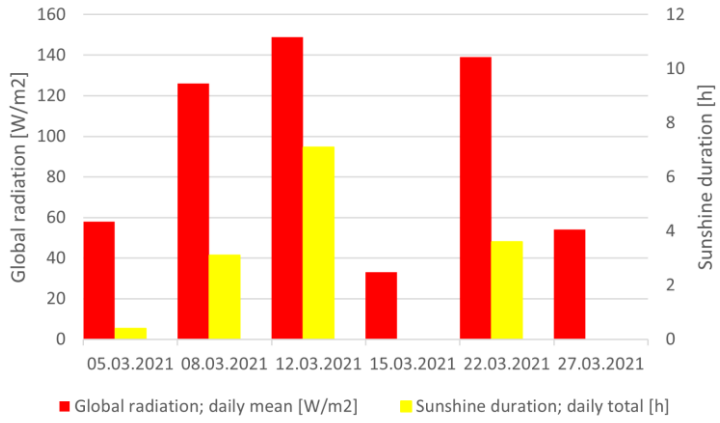

Figure 6: Daily global radiation mean and total sunshine duration for each sampling day

global daily mean radiation and the total sunshine duration for each sampling day. It is visible that on the dates 08.03.2021, 12.03.2021 and 22.03.2021 high global radiation and sunshine duration values were present, relative to the other sampling days.

4.2.6 Wind Direction and Wind Speed

Wind direction and wind speed measurements were taken from the weather station located in Schiers. Since daily total snowfall was measured from 06UTC until 06UTC the following day, wind direction and wind speed were taken from the sampling and the prior day. Wind direction plays a major role in the isotopic composition of snow, as snowfall originating from the leeward side of the mountain causes a positive isotopic lapse rate. Whereas snowfall originating from an orographic effect, will result in a negative isotopic lapse rate. Having wind speed present potentially causes snow drift, which would benefit positive isotopic lapse rates.

The following table (Tab. 3) shows the daily wind direction in degrees and in its cardinal direction, as well as its speed. From the table below, it is visible that during most days wind direction came from Northwest, except for the last sampling day, where the wind showed a direction from Northeast and prior to that day, from the South.

Date	Wind direction; daily mean [°]	Wind direction (cardinal)	Wind speed scalar; daily mean [m/s]
04.03.2021	307	NW	1.4
05.03.2021	318	NW	1.9
07.03.2021	300	NW	1.6
08.03.2021	304	NW	1.5
11.03.2021	315	NW	1.4
12.03.2021	279	W	1.6
14.03.2021	281	W	3
15.03.2021	360	N	1.2
21.03.2021	297	NW	1.7
22.03.2021	300	NW	2
26.03.2021	180	S	1.1
27.03.2021	72	NE	1.2

Table 3: Wind measurements taken from the weather station in Schiers

5 Methods

5.1 Field Work

As mentioned in Chapter 4.1, every altitudinal difference of 100m a snow sample was taken over an elevation gradient of 970m. This was done to ensure that a possible spatial variation in the isotopic composition can be detected in the lab analysis. To control if the sampled snow was not affected by random implications, one to three control samples were taken during the same sampling run. Each control sample was collected on the same elevation but with a fixed distance away from it (2-5m). In the analysis, the control samples were expected to have identical values as their counterparts. Any major deviations would indicate implications due to random variations. All samples were collected with an avalanche shovel (Fig. 7), which was approximately also the size of the area sampled (20x20cm). From these 20x20cm, only the first centimetre layer of fresh snow was taken. The sample was then put in a zip lock bag where the superfluous air was "pressed out". After returning home, the zip lock bag was stored in a refrigerator until the snow melted to prevent further fractionation. As soon as the snow melted, the samples were transferred to vials (Fig. 8) (EcoLine 1.5ml Short Thread Val 32x11.6mm (clear)). In order to ensure that there were no droplets, it was made sure that the zip lock bag was mixed well, before the melted was transferred into the vials. During my sampling run, field notes (Fig. 9) were taken concerning meteorological conditions during my sampling run (snowfall, sunshine, and snow condition). Additionally, my field notes contained information about where and when the sample was taken, which were used to label each vial.

Figure 7: Avalanche shovel and zip lock bag used for each sample run

Figure 8: Vial used for storing snow samples

Date	Sampling Run	Sample Locations	Start	End	Snowfall during night	Snowfall during day	Sunshine during the day	Snow Condition
05.03.2021	S1	4-9	09:39	11:58	Yes	Yes	No	Wet snow
08.03.2021	S2	2-10	10:56	13:56	Yes	No	No	Wet snow
12.03.2021	S3	7-11	09:37	11:05	Yes	No	Yes	Powdery Snow
15.03.2021	S4	3-7	09:35	11:49	Yes	Yes	No	Powdery Snow
22.03.2021	S5	1-11	09:08	12:15	Yes	Yes	No	Wet snow (S5.1-5.3) Powdery snow (S5.4-5.11)
27.03.2021	S6	4-11	09:17	11:54	Yes	Yes	No	Wet snow (S6.4-6.9) Powdery Snow (S6.10-S6.11)

Figure 9: Field notes made during sampling runs

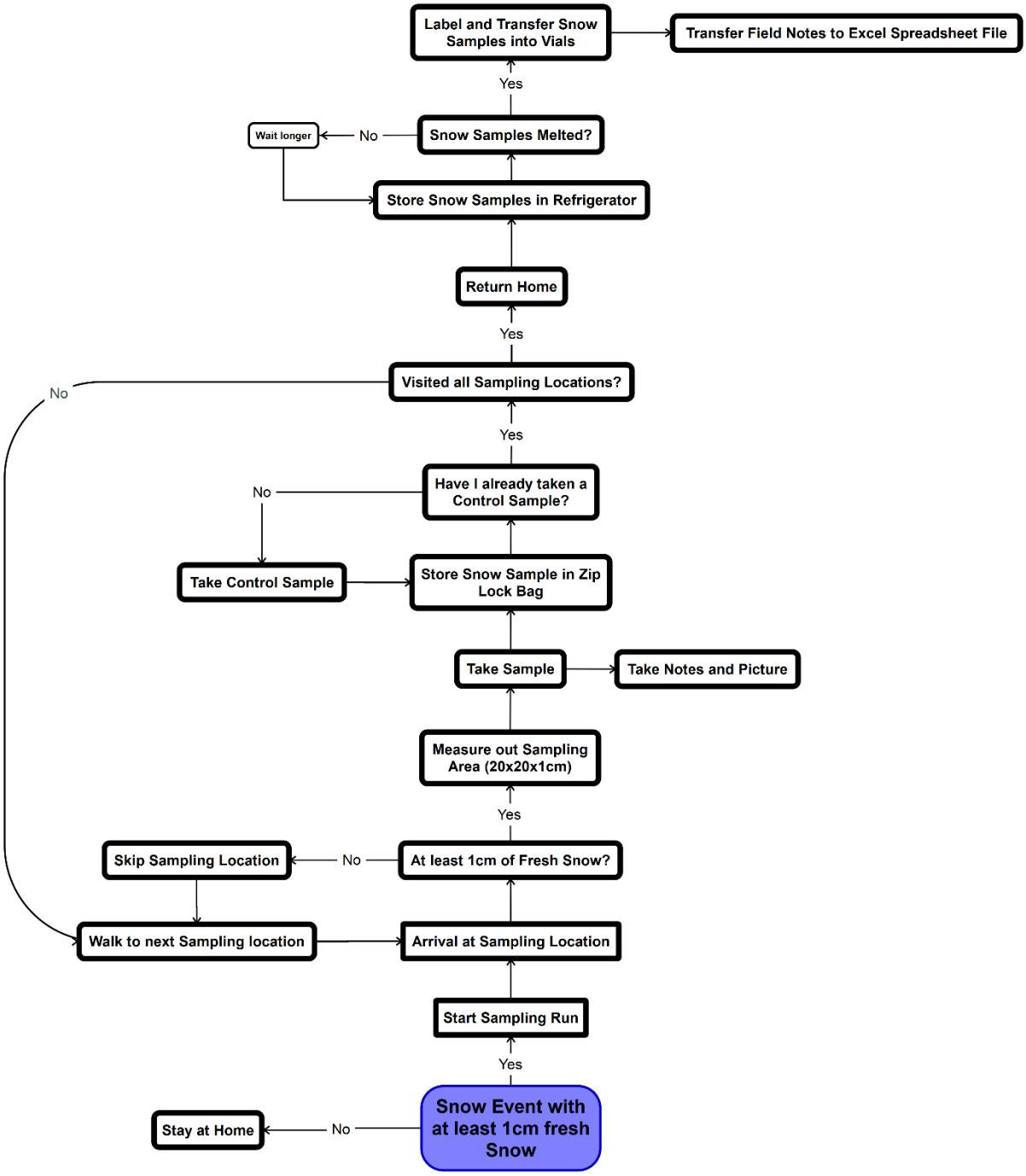

Figure 10: Sampling run depicted as a flow chart

5.2 Lab Work

The analysis of the snow sample was made with a Cavity Ring Down Spectrometer (CRDS) from Picarro (Fig. 11). The CRDS, which was used for this thesis, was the Picarro L2140-*i* isotopic water analyser (figure 8), a laser instrument used for measuring the composition of the isotopes of ^{18}O, ^{17}O and ^{2}H in water samples. My snow samples were always run with the three different water standards ANZO, EMEB and SAAS, which were calibrated in relationship to the standards VSMOW2 by Torsten Venneman. All three water standards are from the laboratory of Torsten Venneman at the University of Lausanne and were provided by my advisor, Natalie C. Ceperley. This means that the values of my samples were measured in reference to the three mentioned water standards, which were needed to determine the $\delta^{18}O$, $\delta^{17}O$ and $\delta^{2}H$ value of my samples. It is worth noting that the Picarro L2140-*i* experiences different guaranteed precision rates for $\delta^{18}O$ (0.04‰ at 300sec), $\delta^{17}O$ (0.04‰ at 300sec) and $\delta^{2}H$-values (0.1‰ at 300sec). The analysis was operated on the 9th of June 2021 in the lab of the Institute of Geography at the University of Berne with the help of my advisor Natalie C. Ceperley.

Figure 11: Cavity Ring Down Spectrometer (CRDS) used at the lab of the Institute of Geography at the University of Berne

5.3 Statistical Analysis

To verify if there is a statistical correlation between the altitude and the isotopic composition of my snow samples, a linear regression analysis was performed with the data analysis tool from Excel. Since the stable water isotopes ^{18}O, ^{2}H and ^{17}O in snow are influenced by many different factors, they were set as the explanatory variables, whereas the altitude was set as the predictor variable. The linear regression analysis was run with a confidence interval of 95%. Therefore, the *p*-value of a sampling run must be <0.05, in order to verify a correlation between the altitude and δ-value of the isotopes, which would then be statistically significant.

6 Results

6.1 Standards δ-Values

Following the analysis with the CRDS, the δ-values of my snow samples were standardized according to calibrated isotope values of the three water standards ANZO, EMEB and SAAS, which are displayed in the table below (Tab. 3).

Standards	δ^2H [‰]	$\delta^{18}O$ [‰]	$\delta^{17}O$ [‰]
ANZO	6.77	1.09	0.59
EMEB	-58.4	-8.14	-4.24
SAAS	-136.31	-18.29	-9.62

Table 3: δ-values of the water standards ANZO, EMEB and SAAS used to standardize my snow samples

6.2 δ^2H-Values

The results for the δ^2H-values for each sampling day are depicted in Figure 12. An enrichment of the heavy isotope ^2H with altitude could be observed throughout the sampling days from the 8th to the 22nd of March, whereas during

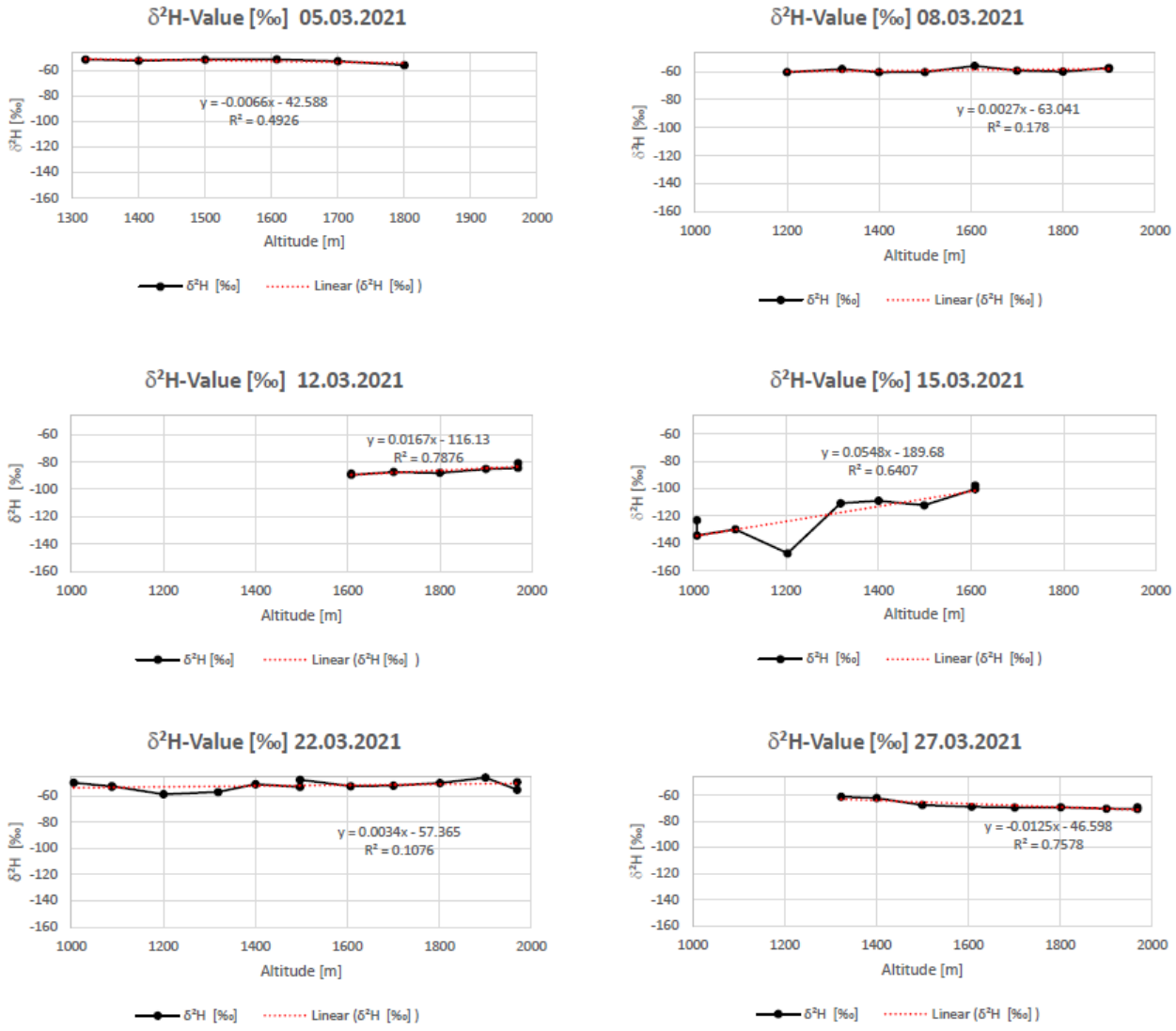

Figure 12: δ^2H-values

the first and the last sampling days, a depletion of ^{2}H with altitude was present. Additionally, one can see that during most of the sampling days, the range of the $\delta^{2}H$-values, reaches from -50‰ to -70‰. However, during the 12th and 15th of March, the snow samples were more depleted in ^{2}H, having δ-values ranging from -80 to -160‰. The results of the days with positive lapse rates show different kinds of altitude gradients, reaching from 0.27‰/100m up to 5.4‰/100m. For the sampling dates with a negative $\delta^{2}H$-lapse rate, the altitude gradients show a lapse rate of -0.66‰/100m and -1.25‰/100m.

A linear regression analysis was run for each sampling day separately, due to the knowledge that every single snowfall shows its own isotopic signature. The results of linear regression analysis with $\delta^{2}H$ as the explanatory variable and the altitude as the predictor variable are listed in table 4. A significant correlation (p <0.05) between the $\delta^{2}H$-values and altitude was determined for the three sampling days on the 12th, 15th and 27th of March, which are depicted in the following table as bold numbers.

Relationship of $\delta^{2}H$ to Elevation

Explanatory Variable: $\delta^{2}H$	05.03.2021	08.03.2021	12.03.2021	15.03.2021	22.03.2021	27.03.2021
R2	0.492	0.178	**0.787**	**0.64**	0.107	**0.757**
p-Value	0.12	0.257	**0.008**	**0.009**	0.252	**0.002**
Slope	-0.0066	0.0027	**0.0167**	**0.0548**	0.0034	**-0.0125**

Table 4: Linear regression results of the explanatory variable $\delta^{2}H$. In bold are the values, which are statistically significant

6.3 $\delta^{18}O$-Values

The results for the $\delta^{18}O$-values are represented in Figure 13. The $\delta^{18}O$-values show similar curves as $\delta^{2}H$ for each respective sampling day. Throughout most of the sampling days the $\delta^{18}O$-values vary from -8‰ to -12‰ with the 15th of March being an outlier, where the $\delta^{18}O$-values reach from -14‰ down to -20‰. The $\delta^{18}O$-lapse rate on the sampling days with a positive lapse rate show an altitude gradient which varies from 0.02‰/100m to 0.64‰/100m. Sampling days with a negative lapse rate show an altitude gradient from -0.05‰/100m to -0.15‰/100m. Alike $\delta^{2}H$, the results of the linear regression analysis with $\delta^{18}O$ as the explanatory variable shows statistically significant *p*-values on the 12th, 15th and 27th of march (Tab. 5).

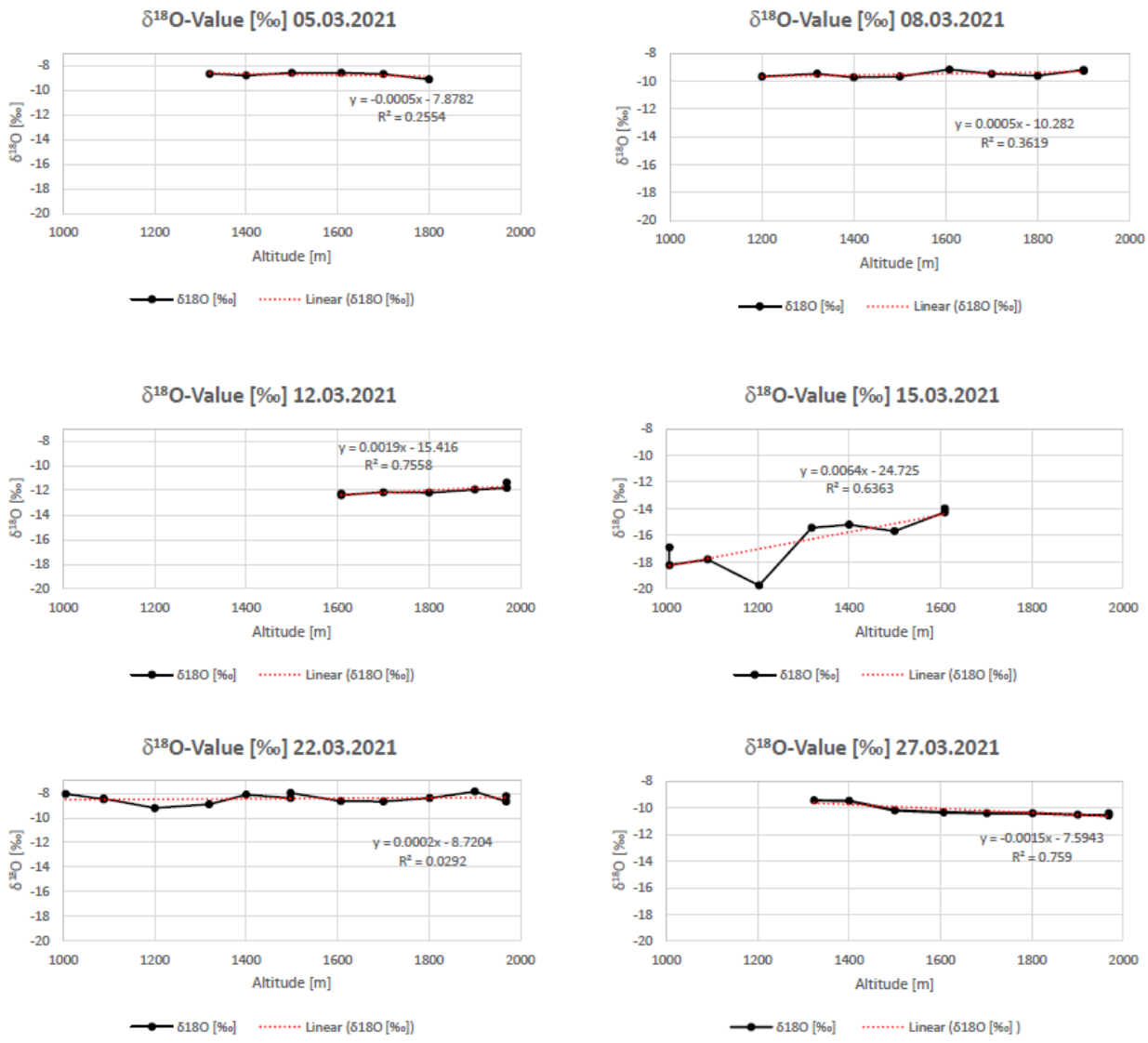

Figure 13: $\delta^{18}O$-values

Relationship of $\delta^{18}O$ to Elevation

Explanatory Variable: $\delta^{18}O$	05.03.2021	08.03.2021	12.03.2021	15.03.2021	22.03.2021	27.03.2021
R2	0.254	0.362	**0.754**	**0.636**	0.029	**0.759**
p-Value	0.38	0.08	**0.024**	**0.01**	0.559	**0.002**
Slope	-0.0005	0.0005	**0.0019**	**0.0064**	0.0002	**-0.0015**

Table 5: Linear regression results of the explanatory variable $\delta^{18}O$. In bold are the values, which are statistically significant

6.4 δ ^{17}O-Values

Like $\delta^{2}H$ and $\delta^{18}O$, $\delta^{17}O$-curve shows a similar trend for each respective sampling day (Fig. 14). Throughout most of the sampling days the δ-values of ^{17}O ranged between -4‰ and -6‰. Except for the 12th and 27th of March. The snow samples on the 12th of March were slightly more depleted in ^{17}O, almost reaching δ-values of -7‰. Like ^{2}H and ^{18}O, ^{17}O showed a relatively strong depletion on the sampling day of the 27th of March, with δ-values ranging from -7‰ down to -11‰.

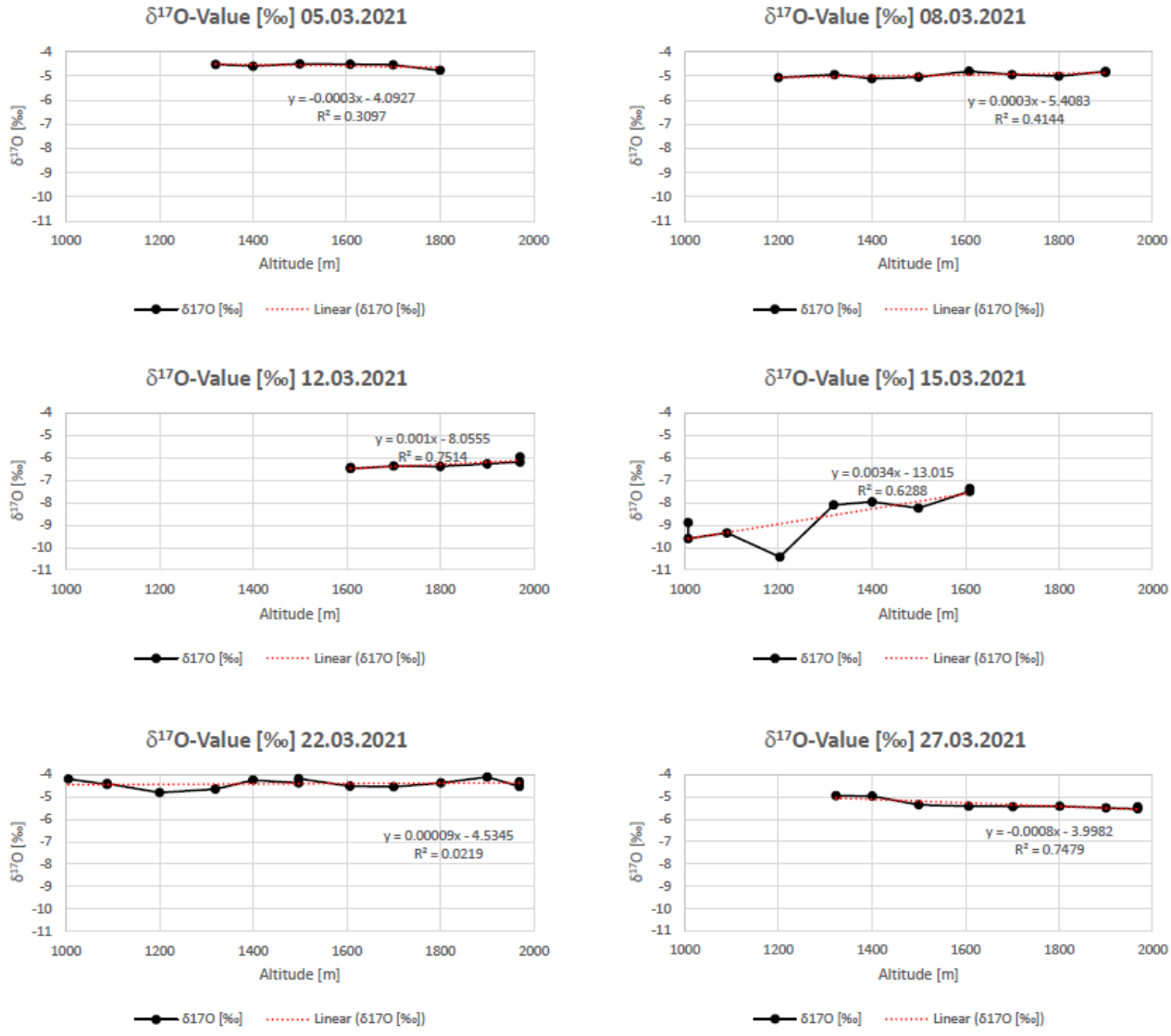

Figure 14: $\delta^{17}O$-values

In comparison to $\delta^{2}H$ and $\delta^{18}O$, $\delta^{17}O$ the isotope lapse rate is much lower. On the sampling days with a positive lapse rate of $\delta^{17}O$ shows an altitude gradient ranging from 0.009‰/100m up to 0.34‰/100m. The lapse rate of $\delta^{17}O$ on the sampling days with a negative lapse rate show a very low altitude gradient of -0.03‰/100m and -

0.08‰/100m. In continuation of δ^2H and $\delta^{18}O$, the results of the linear regression analysis show statistically significant *p*-values and therefore a correlation between the $\delta^{17}O$-values and altitude on the 12th, 15th and 27th of March (Tab. 6).

Explanatory Variable: $\delta^{17}O$	05.03.2021	08.03.2021	12.03.2021	15.03.2021	22.03.2021	27.03.2021
R^2	0.309	0.414	**0.751**	**0.629**	0.021	**0.748**
p-Value	0.251	0.061	**0.011**	**0.01**	0.614	**0.002**
Slope	-0.0003	0.0003	**0.0001**	**0.0034**	0.00009	**-0.0008**

Table 6: Linear regression results of the explanatory variable $\delta^{17}O$. In bold are the values, which are statistically significant

6.5 GMWL and LMWL

Figure 15 illustrates the GMWL (blue line), LMWL (light green line) and the relationship between the δ^2H and $\delta^{18}O$-values of every snow sample collected. The slope of my LMWL (8.5182) only shows a slight difference from the GMWL (8). Interesting is that the intercept of the LMWL of fresh snow seems to be significantly higher (19.884)

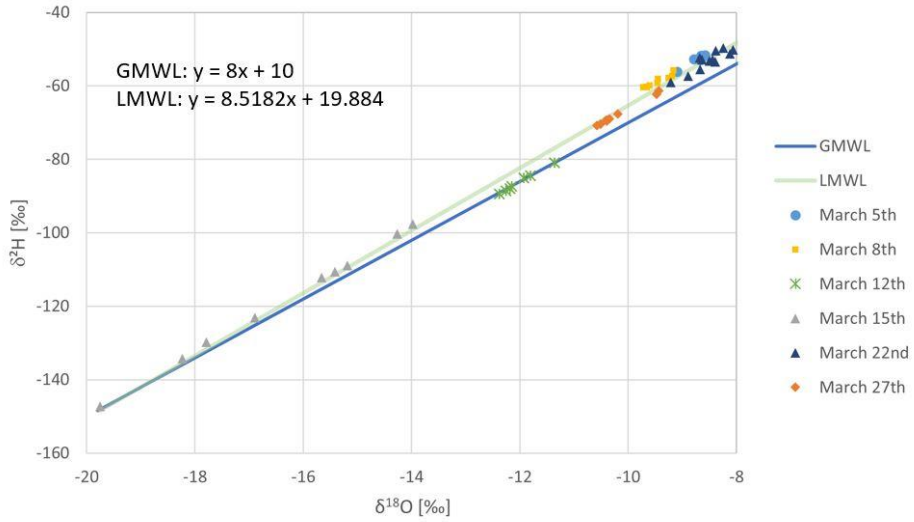

Figure 15: δ^2H-$\delta^{18}O$ plot with their LMWL and GMWL

compared to the GMWL (10). The slight deviation of the slope of my LMWL from the GMWL might just be due to equilibrium processes occurring in a particular temperature range different to the ones in the GMWL. However, since the intercept (or deuterium excess parameter) is significantly higher, it may characterise potential nonequilibrium processes. One possible nonequilibrium process, which leads to a high deuterium excess, is the formation of snow from mixed-phase clouds (see chapter 2). Further data about LMWLs explicitly for precipitation in the form of snow must be collected to determine potential reasons why they might deviate from the GMWL.

6.6 Temperature

Figure 16 illustrates the daily mean $\delta^{18}O$-value plotted against the daily mean temperature. It is visible that there is some kind of trend where $\delta^{18}O$ was less depleted during sampling days with higher temperature compared to sampling days with lower temperatures. If we only consider the mean $\delta^{18}O$-values of the sampling days, which showed a significant altitude gradient, there is a clear trend where isotope fractionation decreases with increasing temperature.

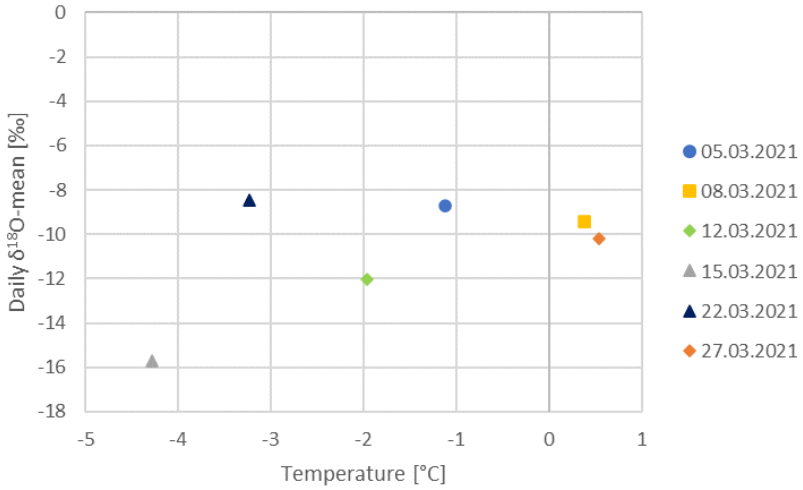

Figure 16: Daily $\delta^{18}O$-mean plotted against mean temperature during snow sampling

6.7 Snowfall Events

Figure 17 depicts the mean $\delta^{18}O$-values of each sampling day and the daily fresh snow measurement from the weather station St.Antoenien over the course from the 1st to the 28th of March. The mean $\delta^{18}O$-value representing

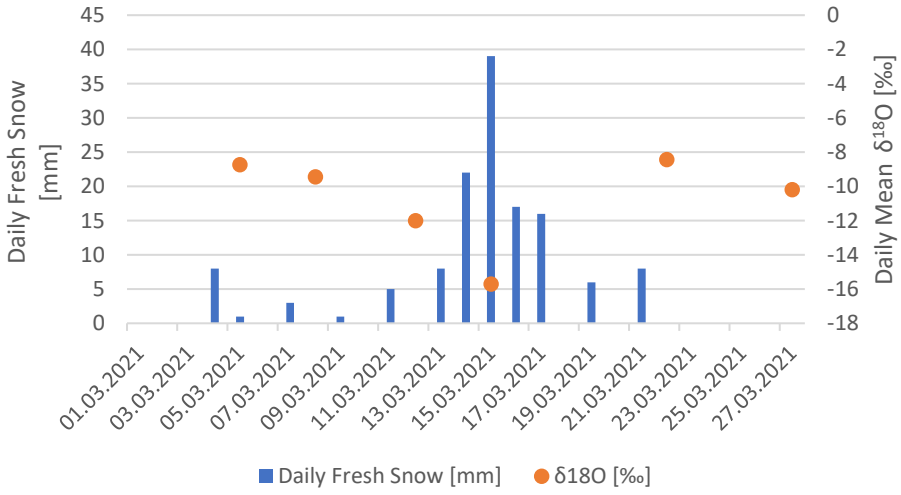

Figure 17: Daily fresh snow measurements from 01.03.2021 until 28.03.2021 plotted against daily mean $\delta^{18}O$-mean of each sampling day

the 27th of March does not correspond with a daily fresh snow bar due to weather station not having measured any snowfall on that day. Figure 17 shows that on the 15th of March, where the duration of the snow event lasted the longest and was the most intense, the snow sample turned out to be most depleted in ^{18}O.

6.8 Solar Radiation

Figure 18 visualizes the $\delta^{18}O$-slope of each sampling day plotted against the daily mean solar radiation. It is visible that the two sampling days, which had shown negative altitude gradients, had relatively low solar radiation compared to the days with a positive altitude gradient. However, the snow samples collected on March 15th had the lowest solar radiation exposure but showed the steepest positive altitude gradient.

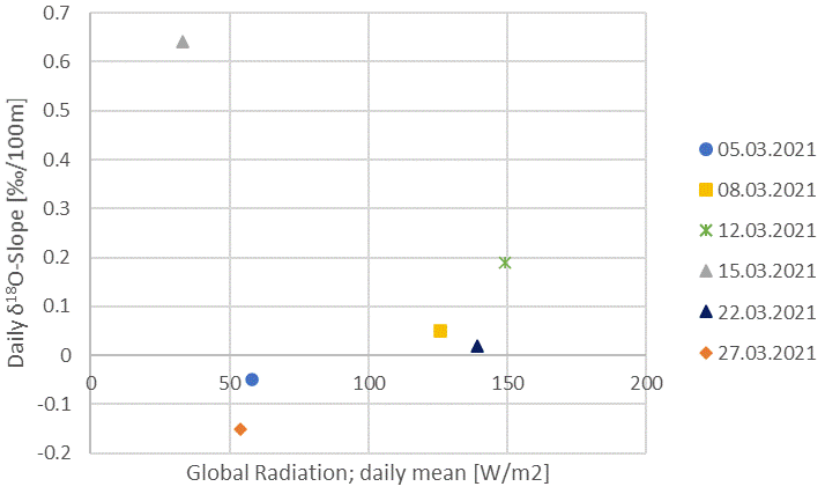

Figure 18: Daily $\delta^{18}O$-slope plotted against daily mean global radiation

6.9 Wind Direction and Speed

Table 7 shows the wind direction and wind speed same as table 2 in chapter 4.2.4 but includes the altitude gradients of $\delta^{18}O$ as well. One can see that during the days where positive altitude gradients were present, wind blew from northwest. However, the sampling day of the 5th of March with a negative altitude gradient also shows a wind direction from northwest. On the other hand, the second sampling day with a negative altitude gradient, on the 27th of March, shows a wind direction from northeast and prior to that day, wind direction from the south.

All of the sampling days show similar wind speeds between 1m/s and 2m/s, with the 14th of March showing a stronger wind speed of 3m/s.

Date	Wind direction; daily mean [°]	Wind direction (cardinal)	Wind speed scalar; daily mean [m/s]	Altitude Gradient $\delta^{18}O$ (‰/100m)
04.03.2021	307	NW	1.4	-
05.03.2021	318	NW	1.9	-0.05
07.03.2021	300	NW	1.6	-
08.03.2021	304	NW	1.5	0.05
11.03.2021	315	NW	1.4	-
12.03.2021	279	W	1.6	**0.19**
14.03.2021	281	W	3	-
15.03.2021	360	N	1.2	**0.64**
21.03.2021	297	NW	1.7	-
22.03.2021	300	NW	2	0.02
26.03.2021	180	S	1.1	-
27.03.2021	72	NE	1.2	**-0.15**

Table 7: Wind measurements from the weather station in Schiers in addition with the altitude gradient of each sampling day

7 Discussion

7.1 The Altitude Effect

A previous study dealing with the altitude effect of δ^2H of snow in the Alps was conducted by Moser and Strichler (1970), where they sampled snow at the end of the accumulation and at the beginning of the ablation period. In their study Moser and Strichler examined an altitude gradient of -3‰/100m with deviations of -2 and -10‰/100m. The results of this study showed only two out of six sampling days with a negative altitude gradient of -0.66‰/100m and -1.25‰/100m. In comparison to the study of Moser and Strichler, the gradients were much lower, which can be traced back to the strong dependency of snow precipitation on meteoric processes currently present, which gives each precipitation event a different isotopic composition. A more recent paper released by Dietermann and Weiler (2013) examined a negative gradient on a south-facing slope in the Eastern Alps ranging between from -1.6‰/100m to -6.2‰/100m. Despite having conducted a very similar study on the same mountain range and on the same exposition, the altitude gradients of Dietermann and Weiler showed very different ranges compared to the ones presented in this thesis. This furthermore shows the strong dependence of the isotopic composition of snow precipitation on meteoric processes.

As seen in the results, four out of six sampling days show an inverse lapse rate, hence an enrichment of heavy isotopes with altitude. In the before mentioned study by Dietermann and Weiler, a positive altitude gradient was examined on the south-facing slopes of their study sites with a range from 0.2‰/100m to 3.1‰/100m. The results of this thesis observed two significant positive altitude gradients, of which one is within the range of Dietermann's and Weiler's study, with a lapse rate of 1.7‰/100m. The statistically second significant altitude gradient was

slightly above the range, with a lapse rate of 5.5‰/100m. The examined altitude effect of δ^2H in this thesis showed different ranges, when compared to results of other studies. However, it is known that δ^2H-values show a wide variation globally (Gat et al., 2001). This would therefore also be the case in this thesis.

In the case of $\delta^{18}O$, this thesis examined two negative altitude gradients of -0.05‰/100m and -0.15‰/100m. However, only the sampling day with the altitude gradient of -0.15‰/100m shows a statistical significance. This gradient does not show any significant difference to other studies, as Gat et. al (2001) report observed isotopic lapse rate between -0.1‰/100m to -0.6‰/100m for globally distributed sites.

Due to the existing relationship between δ^2H and $\delta^{18}O$ defined by the equation $\delta^2H = \delta^{18}O + 10$ (Craig, 1961), $\delta^{18}O$ showed inverse lapse rates in four out of six sampling days as well. Of the four sampling, two altitude gradients have turned out to be of statistical significance with lapse rates of 0.19‰/100m and 0.64‰/100m. A previous study conducted by Moran et al. (2007) examined snow samples for $\delta^{18}O$ in the Canadian Rocky Mountains, where they observed positive altitude gradient during lee-slope precipitation events. Their results show statistically significant positive lapse rates ranging from 0.5‰/100m to 1.8‰/100m. Zongxing et al. (2015) investigated the spatiotemporal evolution of stable isotopes on the Shiyi glacier located in the central Qilian Mountains during the ablation period. The analysis showed a statistically significant positive altitude gradient of 0.876‰/100m in newly deposited snow. A further study by Kong & Pang (2016) observed positive altitude gradients in their precipitation samples on the leeward side of the Tianshan mountains with a relatively low lapse rate of 0.12‰/100m. However, the result presented in this thesis shows a similarly low lapse rate with 0.19‰/100m. Whereas the second statistically significant lapse rate of 0.64‰/100m lies within the range of Moran et. al.

There is still a limited understanding on how the controlling process of the spatiotemporal distribution of ^{17}O work. Additionally, little research has been done on the use of ^{17}O in snow hydrology. It is therefore important to present as much data as possible. In comparison to δ^2H and $\delta^{18}O$, the $\delta^{17}O$-values were much lower, which is not something unconventional. It is known that ^{17}O is a relatively light isotope compared to ^2H and ^{18}O and therefore also more likely to evaporate (Nyamgerel et al., 2021). When directly comparing each sampling day against another, it is visible that the $\delta^{17}O$-values in the snow samples were about half of the $\delta^{18}O$-values, which would therefore also account for the isotopic lapse rate. This would also coincide with previous studies (e.g., Nyamgerel et al., 2021).

7.2 Temperature

According to Berman et al. (2013), the composition of the stable water isotopes ^2H and ^{18}O in precipitation is heavily dependent on temperature. Mook (2001) states a rule of thumb, which says that the isotopic fractionation decreases with increasing temperature. Therefore, precipitation occurring during lower temperature should show a stronger depletion of heavier isotopes compared to precipitation occurring during higher temperatures.

As already mentioned in chapter 6.6, the snow samples in figure 16 show a behaviour where they are more depleted in the heavy isotope ^{18}O during sampling days with lower temperature and less depleted during warmer sampling days. Especially when one would only consider the mean $\delta^{18}O$-values of the days with a statistically significant altitude gradient. This indicates that the rule of thumb set by Mook would then also be applicable for precipitation in the form of snow.

7.3 Snowfall Events

Another factor, which seems to have an influence on the isotopic composition is the length of the duration of a precipitation event (Beria et al., 2018). Beria et al. state that the longer a precipitation lasts, the more depleted in heavier isotopes the precipitation will get. The results depicted in figure 17 only show a vague indication on how the different snow events have influenced the isotopic composition of ^{18}O in my snow samples. But it clearly shows that on the day, where the duration of the snow event lasted the longest and was the most intense, the snow sample turned out to be most depleted in ^{18}O. This would then correspond with the statement of Beria et al., where they state that precipitation is getting more depleted in heavier isotopes the longer it lasts and would therefore also be applicable for snowfall events.

7.4 Solar Radiation

Solar radiation is a major contributor to kinetic fractionation processes in snow. Especially sublimation will be enhanced if high solar radiation is available. As kinetic fractionation processes influence the isotopic composition of snow in a way where it enriches its heavy isotopic content (Beria et al., 2018). Looking back at figure 18 in chapter 6.8, this statement would also be applicable for fresh snow since the sampling days with a relatively high solar radiation output show a positive lapse rate and vice versa. However, the sampling day with the lowest solar radiation output simultaneously presents the day with the steepest altitude gradient. This would indicate that other meteorological conditions must had taken place, which caused a positive altitude gradient.

7.5 Wind Direction and Speed

Depending on whether precipitation in the form of snow or rain falls on the leeward or windward side of the mountain, the isotopic composition of the stable water isotopes and its lapse rate change drastically. Precipitation, which occurred through orographic, preferentially condensates heavy isotopes and therefore leaves the following rain or snowfall more depleted in in heavy isotopes. Since cloud condensation temperature decreases with altitude, a negative isotopic lapse rate comes out as a result. By contrast, if precipitation falls on the leeward side, the isotopic composition is altered by sub-cloud evaporation or moisture recycling, causing an enrichment of heavy isotope with

altitude and hence a positive isotopic lapse rate (Moran et al., 2007). It is therefore important to investigate how the wind direction was when snow sampling was done.

As mentioned in chapter 6.9, days with positive altitude gradients had wind blow from northwest. This would mean that during these days snow also fell on the leeward of the mountain Chruez. Since my study site is located on the southside-slope of the Chruez, positive lapse rates would be expected, which in hindsight, was the case. My results would therefore also coincide with the findings of Moran et. al (2007), Kong & Pang (2016) and Dietermann & Weiler (2013), where they observed positive altitude gradients on leeward sides as well. This would then also add to the observation made in chapter 6.8, where positive lapse rates showed a relatively high solar radiation output. However, the snow samples of the sampling day on the 5th of March shows a negative altitude gradient, despite having wind coming from northwest. One possible explanation could be that the effect of solar radiation outweighed the effect of the leeward side snowfall. Looking back at figure 18 in chapter 6.8, it is visible that on that day, solar radiation was relatively low and therefore may had caused little to no sublimation, which would benefit a negative altitude gradient. Contrary, the fact that wind blew directly from the north may explain why the snow samples on the 15th of March showed a negative lapse rate, despite having the lowest solar radiation output of all the sampling days. On the other hand, the second sampling day, which exhibits a negative altitude gradient, experienced a clear wind direction from the south prior and a wind direction coming from northeast during the sampling day. Due to my field notes stating that snowfall occurred during night-time and my meteorological data measuring fresh snowfall from 06UTC until 06UTC the following day, it is most likely that some of the following precipitation occurred due to orographic process. This could be a possible explanation for the examined negative lapse rate in addition with the relatively low solar radiation output during the sampling day.

Since all of the sampling days show similar wind speeds between 1m/s and 2m/s, there might have been snow drift present. However, since there are no significant differences, the effect of wind speed on the isotopic composition and lapse rate of the snow samples is most likely negligible for this study.

7.6 Error Sources

7.6.1 Field Work

Potential error sources start with the sampling of my snow samples. During some sample runs it was difficult to distinguish between old and new snow layers. Therefore, it may had been the case that in some instances I accidentally also dug up old snow as well. Additionally, throughout most of my sampling runs, wet snow conditions were present and since snowfall also always occurred during night-time, there may have been moments where precipitation fell in the form of rain. Meaning that my results are not fully applicable for fresh snow.

In order to prevent any further fractionation processes of my samples, I tried to “squeeze” the remaining air out of the zip lock bags as good as possible. However, it is most likely that there was still air remaining within the zip lock bags, which could had triggered further isotopic fractionation during the melting process of my snow samples.

7.6.2 Lab Work

My first sampling run was done on the 5th of March, while the actual analysis in the lab was done approximately three months later, on the 9th of June. The time between my first sampling run and measuring the δ-values in the lab surely had an impact on the isotopic composition of my snow samples, which is why my results do not fully represent δ-values for fresh snow. In chapter 5.1, I stated that any deviations in the δ-values of the control sample from the reference sample are due to implications of random variations. Small deviations may also be from the different guaranteed precision rates of the CRDS. However, the control samples 3.11, 4.1, 4.7 and 5.11 show large deviations from the δ^2H-values of its reference sample (Tab.8), which are most likely attributed to mistakes I made during sampling, labelling and/or standardizing. Therefore, it is important to use the results of this thesis with caution.

Sample Name	Deviation δ^2H-values [‰]	Deviation δ^{18}O-values [‰]	Deviation δ^{17}O-values [‰]
2.10 / Control	0.50	0.07	0.04
3.7 / Control	0.86	0.12	0.05
3.11 / Control	-3.49	-0.45	-0.23
4.1 / Control	11.18	1.34	0.72
4.7 / Control	-2.66	-0.29	-0.14
5.2 / Control	-0.30	-0.06	-0.04
5.5 / Control	0.13	0.27	2.20
5.11 / Control	-5.88	-0.43	-0.21
6.10 / Control	0.28	0.06	0.04

Table 8: Deviations from the δ-values of the control samples to the reference samples

7.6.3 Meteorological Data

Since the isotopic composition of any kind of precipitation is heavily influenced by local meteorological conditions, appropriate meteorological data allows for further understanding of variations in values. The meteorological data used for this thesis do not represent the meteorological condition during my sampling days, though they were extracted from weather stations located near my study site. Additionally, there are also differences visible when comparing the meteorological data with my field notes. For example, on the 27th of March the weather station in St.Antoenien did not register a snowfall event. However, my field notes state that there was snowfall during the day. On top of that, the meteorological data is not directly applicable for the whole study site due to it only being measurements representing a location at a specific altitude. Therefore, it is difficult to assume how the meteorological conditions varied over different altitudes.

8 Conclusion

To better understand how the composition of the stable water isotopes ^{2}H, ^{18}O and ^{17}O vary spatially in fresh snow, I sampled stable water isotopes during six different snowfall events in the month of March. In order to get a further understanding on what might had affected the stable water isotope composition of my snow samples, meteorological data including temperature, snowfall, solar radiation, wind direction and wind speed was downloaded from the MeteoSwiss ground level monitoring network archive. Since two out of six sampling days turned out to have statistically significant positive altitude gradient and only one sampling day showed a significant negative altitude gradient, my initial hypothesis was only partly confirmed. While it seems that solar radiation and wind direction impacted the isotopic composition of my snow samples in a way in which it caused either a positive or negative altitude gradient, concrete statements cannot be made, since the meteorological data used for the interpretation does not represent my study site. The same goes for the interpretation of the impact of the temperature and fresh snow measurements on the isotopic composition of my snow samples. My temperature measurements were only an approximation through a self-made calculation and fresh snow measurement was taken from a location, which did not even show a southern exposition. Additionally, with the limited knowledge about LMWLs of snow, it is very difficult to give a clear interpretation about what the deviations of my LMWL ($y = 8.5182x + 19.884$) from the GMWL ($y = 8x + 10$) might indicate in terms of isotope fractionation processes. Therefore, the follow up hypothesis can be discarded.

This bachelor thesis shows the importance of further research in the field of the isotopic composition of fresh snow to determine what kind of meteorological conditions or processes affect it and in order to get a clearer and deeper understanding on how the hydrological cycle works.

8.1 Future Research

For future research I recommend equipping oneself on sampling runs with instruments measuring air temperature, relative humidity, wind direction and speed. In order to evaluate the accuracy of the instruments, one could compare these data with nearby weather stations and assess how much they deviate. An alternative would be to collect snow samples within sites, which have weather stations available. Stable water isotopes are heavily influenced by meteorological conditions and thus, having the most accurate meteorological data available is of the essence.

It would have been interesting to not only investigate the spatial but also the temporal variation of stable water isotopes in fresh snow, be it during the same sampling day or at a different point and time during the winter season. As stated by Nyamgerel et al. (2021), there is still little knowledge about ^{17}O's place within the hydrological cycle, which makes continuous research about its spatiotemporal behaviour all the more important. There is also the lack of knowledge about LMWLs for fresh snow, since most LMWLs are only applicable for precipitation in the form

of rain. It is therefore important to accumulate as much fresh snow data as possible and compare its LMWLs, which may give better insights on what kind of processes affect the isotopic composition of snow precipitation.

References

Ambach, W., Dansgaard, W., Eisner, H., & Møller, J. (1968). The altitude effect on the isotopic composition of precipitation and glacier ice in the alps. *Tellus, 20,* 595-600. https://doi.org/10.3402/tellusa.v20i4.10040

Berie, H., Larsen, R.J., Ceperley, N.C., Michelon, M., Vennemann, T., & Schaefli, B. (2018). Understanding snow hydrological processes through the lens of stable water isotopes. *WIREs Water, 5.*

Berman, E.S.F., Levin, N.E., Landais, A., Li, S., & Owano, T. (2013). Measurement of $\delta^{18}O$, $\delta^{17}O$, and ^{17}O-excess in Water by Off-Axis Integrated Cavity Output Spectroscopy and Isotope Ratio Mass Spectometry. *Analytical Chemistry, 85,* 10392-10398. https://doi.org/10.1021/ac402366t

Bershaw, J., Hansen, D.D., & Schauer, J.A. (2020) Deuterium excess and ^{17}O-excess variability in meteoric water across the Pacific Northwest, USA. *Tellus B: Chemical and Physical Meteorology, 72,* 1-17. https://doi.org/10.1080/16000889.2020.1773722

Ceperley, N.C., Zuecco, G., Beria, H., Carturan, L., Michelon, A., Penna, D., Larsen, J., & Schaefli, B. (2020). Seasonal snow cover decreases young water fractions in high Alpine catchments. *Hydrological Processes, 34,* 4794-4813. https://doi.org/10.1002/hyp.13937

Cooper, L.W. (1998). Isotopic Fractionation in Snow Cover. In: Kendall, C., & McDonnell, J.J. (Eds.). *Isotope tracers in catchment hydrology,* 119-131. Netherlands. Elsevier.

Craig, H. (1961). Isotopic Variations in Meteoric Waters. *Science, 133,* 1702-1703. https://doi.org/10.1126/science.133.3465.1702

Dietermann, N., & Weiler, M. (2013). Spatial distribution of stable water isotopes in alpine snow cover. *Hydrology and Earth System Sciences, 17,* 2657-2668. https://doi.org/10.5194/hess-17-2657-2013

Gat, J.R., Mook, W.G., & Meijer, H.A.J. (2001). Observed Isotope Effects in Precipitation. In: Gat, J.R., Mook, W.G., & Meijer, H.A.J. (Eds). *Environmental Isotopes in the Hydrological Cycle Volume 2: Principles and Applications,* 197-203, International Atomic Energy Agency and United Nations Educational, Scientific and Cultural Organization.

Galewsky, J., Stehen-Larsen, H.C., Field, R.D., Worden, J., Risi, C., & Schneider, M. (2016). Stable isotopes in atmospheric water vapor and logic cycle. *Revies of Geophysics, 54,* 809-865. https://doi.org/10.1002/2015RG000512

Gustafson, J.R., Brooks, P.D., Molotch, N.P., & Veatch, W.C. (2010). Estimating snow sublimation using natural chemical and isotopic tracers across a gradient of solar radiation. *Water Resources Research, 46.* https://doi.org/10.1029/2009WR009060

Hoefs, J. (2015). *Stable Isotope Geochemistry*. Springer. Cham.

Kendall, C., & McDonnell, J.J. (1998). *Isotope tracers in catchment hydrology.* Netherlands. Elsevier.

Kern, Z., Kohán, B., & Leuenberger, M. (2014). Precipitation isoscape of high reliefs: interpolation scheme designed and tested for monthly resolved precipitation oxygen isotope records of Alpine domain. *Atmospheric Chemistry and Physics, 14,* 1897-1907. https://doi.org/10.5194/acp-14-1897-2014

Kong, Y., & Pang, Z. (2016). A positive altitudinal gradient of isotopes in the precipitation over the Tianshan Mountains: Effects of moisture recycling and sub-cloud evaporation. *Journal of Hydrology, 542,* 222-230. https://doi.org/10.1016/j.jhydrol.2016.09.007

Kumar, S.U., Kumar, B., Rai, S.P., & Sharma, S. (2010). Stable isotope ration in precipitation and their relationship with meteorological conditions in the Kumaon Himalayas, India. *Journal of Hydrology, 391,* 1-8. https://doi.org/10.1016/j.jhydrol.2010.06.019

Michelon, A., Ceperley, N., Beria, H., Larsen, J., & Schaefli, B. (2018). Quantification of snowmelt processes in a high Alpine catchment from hydrographs, satellite images and stable water isotopes. *Geophysical Research Abstracts, 20*.

Mook, G.W. (2001): *Environmental Isotopes in the Hydrological Cycle Volume 2: Principles and Applications*. International Atomic Energy Agency and United Nations Educational, Scientific and Cultural Organization.

Moran, T.A., Marshall, S.J., Evan, E.C., & Sinclair, K.E. (2007). Altitude gradients of stable isotopes in lee-slope precipitation in the Canadian Rocky Mountain, *Arctic, Antarctic, and Alpine Research, 39,* 455-467. https://doi.org/10.1657/1523-0430(06-022)[MORAN]2.0CO;2

Nyamgerel, Y., Han, Y., Kim, M., Koh, D., & Lee, J. (2021). Review on Applications of ^{17}O in Hydrological Cylce, *Molecules, 26.* https://doi.org/10.3390/molecules26154468

Peng, T.R., Chen, K.Y., Zhan, W.J., Lu, W.C., & John Tong, L.T. (2015). Use of stable water isotopes to identify hydrological processes of meteoric water in montane catchmentes. *Hydrological Processes, 29,* 4957-4967. https://doi.org/10.1002/hyp.10557

Putman, A.L., Fiorella, R.P., Bowen, G.J., & Cai, Z. (2019). A Global Perspective on Local Meteoric Water Lines: Meta-analytic Insight into Fundamental Controls and Practical Constraints. *Water Resources Research, 55,* 6896-6910. https://doi.org/10.1029/2019WR025181

Schotterer, U., Schürch, M., & Rickli, R. (2010). Water Isotopes in Switzerland. Latest Findings of the National ISOT Network. *Gas Wasserfach Wasser Abwasser, 12,* 1073-1081.

Schürch, M., Kozel, R., & Schotterer, U. (2003). Observation of Isotopes in the Water Cycle – the Swiss National Network (NISOT). *Environmental Geology, 45,* 1-11. 10.1007/s00254-003-0843-9

Vreča P., & Kern, Z. (2020). Use of Water Isotopes in Hydrological Processes. *Water, 12,* 2227. https://doi.org/10.3390/w12082227

Zongxing, L., Qi, F., Tingting, W., Xiaoyan, G., Zongjie, L., Yan, G., Yanhui, P., Rui, G., Bing, J., Yaoxau, S., & Chuntan, H. (2015). The stable isotope evolution in Shiyi glacier system during the ablation period in the north of Tibetan Plateu, China. *Quaternary International, 380-381,* 262-271. https://doi.org/10.1016/j.quaint.2015.02.013